Determination of Molecular Structure of Bisphenylene Homologues of BINOL-Based Phosphoramidites by Chiroptical Methods

Ondřej Julínek,[†] Vladimír Setnička,[†] Natalia Miklášová,[‡] Martin Putala,[‡] Kenneth Ruud,[§] and Marie Urbanová*[,∥]

Department of Analytical Chemistry and Department of Physics and Measurements, Institute of Chemical Technology, Prague, Technická 5, 166 28 Prague 6, Czech Republic, Department of Organic Chemistry, Faculty of Natural Sciences, Comenius University in Bratislava, Mlynská dolina, 842 15 Bratislava, Slovak Republic, and Centre for Theoretical and Computational Chemistry, Department of Chemistry, University of Tromsø, N-9037 Tromsø, Norway

Received: July 16, 2009; Revised Manuscript Received: August 27, 2009

Vibrational (VCD), electronic circular dichroism (ECD), and IR absorption spectra together with transparent spectral region optical rotation (OR) of two derivatives of bisphenylene 1,1′-binaphthyl-based phosphoramidites containing three stereogenic axes were measured and the results were compared with simulated data obtained by ab initio calculations with density functional theory. An excellent agreement between experimental and predicted B3LYP/6-31G** and BPW91/6-31G** VCD spectra enabled the assignment of all VCD bands in the experimental spectra, while the Gibbs free energy of all the conformers allowed the determination of their relative populations. The calculation of ECD spectra showed that CAM-B3LYP/6-311G** provided results superior to those of B3LYP/6-311G**. The theoretical results for the OR at the B3LYP/6-311G** and CAM-B3LYP/6-311G** levels were in good agreement with experimental optical rotations, but exhibited lower sensitivity in determining particular conformers than VCD and ECD. By a careful comparison of experimental VCD, IR, and ECD spectra and OR with calculated data, it was possible to assign the absolute configuration of all three stereogenic axes and to determine the molecular structure of the studied bisphenylene 1,1′-binaphthyl-based phosphoramidites in solution with a high degree of confidence.

Introduction

Among the extensive group of chiral molecules, 1,1′-binaphthyl-2,2′-diol (BINOL) is a typical representative possessing axial chirality. When separated as a single enantiomer, it represents an excellent building block for the preparation of catalysts for many important stereoselective reactions, such as asymmetric oxidation and reduction or asymmetric C−C bond forming reactions.[1] Its derivatives, BINOL-based phosphoramidites, can be used as ligands in enantioselective organic reactions: copper-catalyzed alkylations of imines[2] and activated alkenes (conjugated addition),[3,4] palladium- and nickel-catalyzed hydrovinylations of alkenes,[5] or asymmetric rhodium-catalyzed hydrogenation of alkenes.[6] In this work, we perform a structural study of bisphenylene homologues of BINOL-based phosphoramidites, whose absolute configuration at the naphthyl−naphthyl stereogenic axis is given by the synthesis (Scheme 1).

To study the structure of BINOL derivatives in solution and determine their absolute configuration, several chiroptical methods can be utilized. When the only purpose of the work is to distinguish between two enantiomers, it is possible to employ transparent spectral region optical rotation (OR), which seems to work well for the determination of absolute configurations of simple binaphthols.[7] However, when the molecule contains more than one stereogenic center, the relative configuration of which is not known, this method becomes insufficient. Because of the exciton coupling phenomenon caused by the presence of proximal naphthyl chromophores, it is possible to use electronic circular dichroism (ECD) spectroscopy, as the spectrum of binaphthyl derivatives strongly depends on the dihedral angle between naphthyl planes.[8,9] In addition, when more than two stereogenic centers are present in the molecule, the determination of their absolute configurations by ECD can be difficult, especially when electronic transitions are not well-resolved in the spectrum. Furthermore, the results of an ECD study can be ambiguous, as the calculated spectrum strongly depends on the type and parametrization of the profile curve[10] and can be slightly shifted in the excitation energies with respect to experiment. Hence it seems appropriate to employ vibrational

SCHEME 1: Structure of Bis-*o*-phenylene (ORTHO) and Bis-*m*-phenylene (META) Homologues of BINOL-Based Phosphoramidites[a]

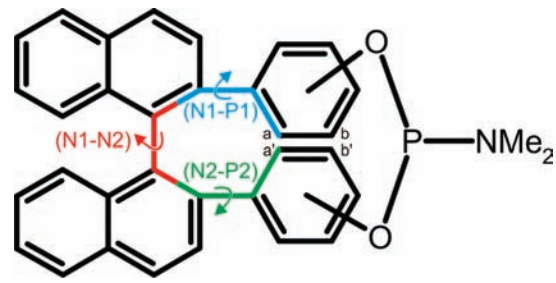

[a] Important dihedral angles are color-coded. The phosphoramidite group is connected to the phenyl rings in positions a, a′ and b, b′ for **ORTHO** and **META**, respectively.

* To whom correspondence should be addressed. E-mail: marie.urbanova@vscht.cz.
[†] Department of Analytical Chemistry, Institute of Chemical Technology.
[‡] Comenius University in Bratislava.
[§] University of Tromsø.
[∥] Department of Physics and Measurements, Institute of Chemical Technology.

10.1021/jp906724f CCC: $40.75
Published on Web 09/16/2009

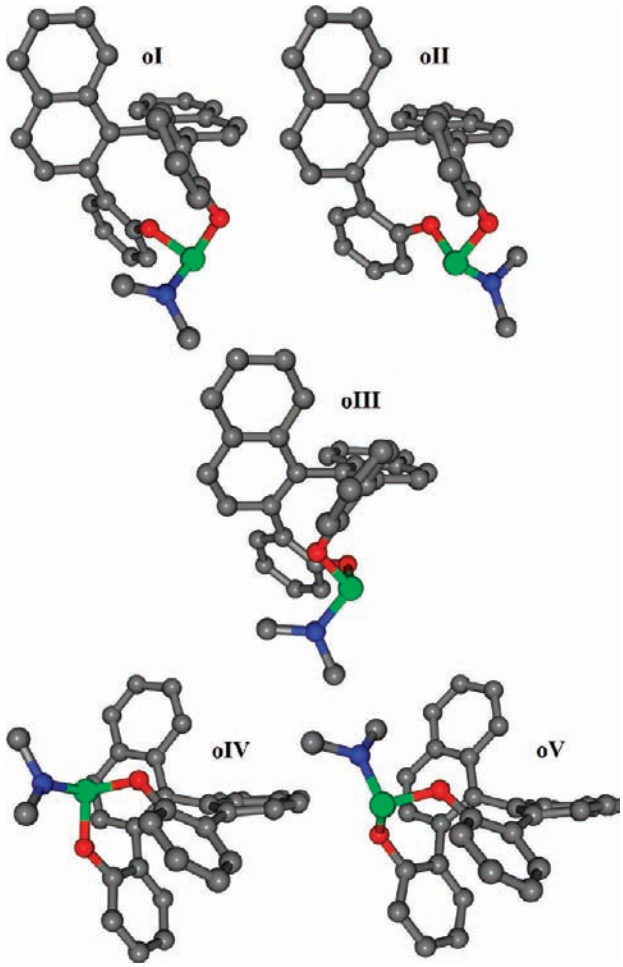

Figure 1. BPW91/6-31G** structures of the conformers of **ORTHO**. Hydrogen atoms are omitted for clarity.

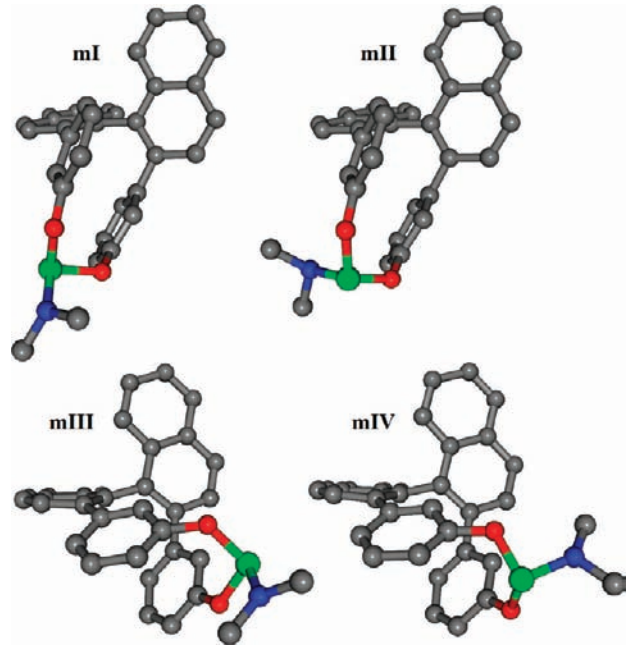

Figure 2. BPW91/6-31G** structures of the conformers of **META**. Hydrogen atoms are omitted for clarity.

circular dichroism (VCD), which has been shown to be able to determine absolute configurations of various molecules[11] by a comparison of an experimental spectrum with the spectrum calculated by using Stephens' magnetic field perturbation theory together with gauge-including atomic orbitals.[12] VCD provides detailed information about a chiral molecule: the configuration of its chiral centers, the spatial arrangement, as well as the interaction with other molecules. A successful utilization of this chiroptical method for the study of binaphthyl derivatives has already been reported.[7,13]

The goal of this work was to determine the configurations of all stereogenic axes of two binaphthyl derivatives, bis-*o*-phenylene (abbreviated as **ORTHO**) and bis-*m*-phenylene (abbreviated as **META**) homologues of BINOL-based phosphoramidites (Scheme 1) (which can influence their catalytic activity), to disclose all possible conformers and estimate their relative abundance in solution. The results of this study will help us to determine whether bisphenylene BINOL-phosphoramidites exhibit any difference in conformational behavior that could affect the catalytic function of these molecules compared to that of noncyclic binaphthyls. To achieve all these objectives, an approach in which experimental ECD, VCD, IR, and OR methods, the combination of which greatly improves the reliability of the structural results,[14] is applied together with ab initio calculations.

TABLE 1: The Equilibrium Population of the Conformers of ORTHO Derived from Relative Free Energies (Δ*G*) Calculated at the B3LYP/6-31G and BPW91/6-31G** Levels**

	B3LYP/6-31G**				BPW91/6-31G**			
conformer	Δ*E* (kJ/mol)	population (%)	Δ*G* (kJ/mol)	population (%)	Δ*E* (kJ/mol)	population (%)	Δ*G* (kJ/mol)	population (%)
oI	0.0	81.2	0.0	84.7	0.0	85.6	0.0	86.1
oII	3.7	18.4	4.3	15.1	4.5	14.1	4.6	13.7
oIII	13.3	0.4	14.9	0.2	14.2	0.3	15.7	0.2
oIV	71.8	0.0	75.0	0.0	63.6	0.0	66.9	0.0
oV	88.2	0.0	89.9	0.0	81.2	0.0	85.4	0.0

TABLE 2: Dihedral Angles at Naphthyl−Naphthyl, Naphthyl(1)−Phenyl(1), and Naphthyl(2)−Phenyl(2) Stereogenic Axes (denoted as (N1−N2), (N1−P1), and (N2−P2), respectively) of the Conformers of ORTHO Calculated at the B3LYP/6-31G and BPW91/6-31G** Levels**

		B3LYP/6-31G**			BPW91/6-31G**		
conformer	configuration	dih(N1−N2)	dih(N1−P1)	dih(N2−P2)	dih(N1−N2)	dih(N1−P1)	dih(N2−P2)
oI	(*R*,*S*,*S*)	−96.0	123.2	75.7	−96.1	124.5	73.3
oII	(*R*,*S*,*S*)	−98.7	114.7	59.6	−98.6	115.3	58.8
oIII	(*R*,*S*,*S*)	−108.7	61.8	55.2	−109.6	60.7	53.9
oIV	(*R*,*R*,*S*)	−76.0	−48.6	101.9	−75.2	−47.1	103.6
oV	(*R*,*R*,*S*)	−77.0	−54.2	110.2	−76.3	−52.6	111.6

TABLE 3: The Equilibrium Population of the Conformers of META Derived from Relative Free Energies (ΔG) Calculated at the B3LYP/6-31G and BPW91/6-31G** Levels[a]**

	B3LYP/6-31G**				BPW91/6-31G**			
conformer	ΔE (kJ/mol)	population (%)	ΔG (kJ/mol)	population (%)	ΔE (kJ/mol)	populatiom (%)	ΔG (kJ/mol)	population (%)
mI	0.0	100.0	0.0	100.0	0.0	100.0	0.0	100.0
mII	29.0	0.0	33.5	0.0	32.4	0.0	35.4	0.0
mIII	68.7	0.0	74.0	0.0	63.2	0.0	66.9	0.0
mIV	NA	NA	NA	NA	63.2	0.0	63.9	0.0

[a] NA means that the conformer is not an energetic minimum at the declared level of theory.

TABLE 4: Dihedral Angles at Naphthyl−Naphthyl, Naphthyl(1)−Phenyl(1), and Naphthyl(2)−Phenyl(2) Stereogenic Axes (denominated as (N1−N2), (N1−P1), and (N2−P2), respectively) of the Conformers of META Calculated at the B3LYP/6-31G and BPW91/6-31G** Levels[a]**

		B3LYP/6-31G**			BPW91/6-31G**		
conformer	configuration	dih(N1−N2)	dih(N1−P1)	dih(N2−P2)	dih(N1−N2)	dih(N1−P1)	dih(N2−P2)
mI	(*S*,*R*,*R*)	77.2	−117.0	−109.6	75.6	−117.3	−111.8
mII	(*S*,*R*,*R*)	75.9	−114.8	−112.7	74.7	−115.8	−113.8
mIII	(*S*,*S*,*R*)	86.3	26.3	−110.7	85.7	25.7	−111.3
mIV	(*S*,*S*,*R*)	NA[a]	NA	NA	86.7	21.9	−115.7

[a] NA means that the conformer is not an energetical minimum at the declared level of theory.

Experimental Methods

Bis-*o*- and bis-*m*-phenylene homologues of BINOL-based phosphoramidites (Scheme 1) were synthesized and characterized by the methods described elsewhere.[15] $CDCl_3$ (99.8% D) used as a solvent for IR and VCD measurements was purchased from Isosar GmbH (Germany). Analytical grade $CHCl_3$ from Lachner (Czech Republic) was used for ECD and OR measurements.

The IR absorption and VCD spectra of $CDCl_3$ solutions of **ORTHO** and **META**, both at a concentration of 70.3 g L^{-1} (0.13 mol L^{-1}), were measured by using a Bruker IFS-66/S FT-IR spectrometer equipped with a PMA 37 VCD/IRRAS module (Bruker, Germany) as described previously.[16] A demountable cell A145 (Bruker, Germany) constructed of KBr windows separated by a 210 μm Teflon spacer was used for all measurements. The spectral resolution was 4 cm^{-1} and the zero-filling factor was 4. The final VCD spectra were averaged from 16 blocks, each of 2260 interferometric scans accumulated for 20 min. Baseline correction using the spectra of the solvent obtained under the same experimental conditions was performed.

The ECD spectra of **ORTHO** and **META**, both at a concentration of 0.51 g L^{-1} (1.0 mM) in $CHCl_3$, were recorded with a Jasco J-810 spectropolarimeter (Japan) and a 0.1 mm quartz cell, with a 1 nm bandwidth, a time constant of 2 s, and a scanning speed of 50 nm min^{-1}. Four blocks of scans were recorded, averaged, and baseline-subtracted by using a spectrum of the solvent.

Optical rotations of $CHCl_3$ solutions of **ORTHO** (3.18 g L^{-1}) and **META** (2.42 g L^{-1}) were measured on an AUTOPOL IV polarimeter (Rudolph Research Analytical, USA), at 365, 405, 436, 546, 589, and 633 nm and 20 °C.

Calculations

Conformational analysis of the *o*- and *m*-binaphthyl derivatives was accomplished by the conformational search module of the HyperChem 8 software package,[17] using the MM+ force field. Initial geometries of both BINOL derivatives had a predefined absolute configuration of the naphthyl−naphthyl stereogenic axis, and although the conformational search process was allowed to change all dihedral angles within the cyclic structure, the inversion of this central stereogenic axis was disabled. However, because of the possibility of a limited rotation along both of the naphthyl−phenyl stereogenic axes, a change in their absolute configuration during the conformational search was possible. Final optimization of all structures as well as the calculation of VCD and IR absorption spectra was carried out with the Gaussian 03 software[18] at the DFT level of theory. We have used the 6-31G** basis set throughout this work in conjunction with the generalized-gradient approximation (GGA) exchange-correlation (XC) functional BPW91, which has been shown to give reliable simulations of VCD spectra of various binaphthyl derivatives,[13] and the hybrid B3LYP (XC) functional, the latter because it is a standard method for the calculation of VCD spectra. The calculation of ECD spectra and optical rotations was done with use of the Dalton software.[19] The B3LYP and CAM-B3LYP[20] functionals were used throughout, together with the 6-311G** basis set. B3LYP was chosen since it is the de facto standard functional, whereas the CAM-B3LYP functional was utilized since it was recently reported to provide superior results for calculations of electronic transitions in some systems, especially conjugated molecules with charge transfer excitations.[21−26]

The equilibrium population of all conformers at $T = 293.15$ K was estimated according to their calculated ΔG values, which were calculated at the same level as VCD spectra and included zero-point energy and vibrational, rotational, and translational thermal energy corrections. VCD and IR absorption spectra were plotted assuming a Lorentzian band shape with a 5 cm^{-1} half-width of the peak, well matching the broadening of the VCD bands in the experimental spectra. In the case of VCD and IR absorption spectra calculated with use of the B3LYP functional, all transitions were scaled by a factor of 0.93, which provided the best agreement in the position of most experimental and calculated bands in the spectrum; for BPW91 no scaling factor was needed. ECD spectra were plotted assuming a Gaussian band shape with a 0.35 eV full-width at half-maximum, approximately matching the broadening of the ECD bands in the experimental spectra. DFT calculations were carried out on an Altix 350 computer (Silicon Graphics) at the Computer Center of ICT Prague, and on a Cluster Platform 3000 BL460c (Hewlett-Packard) at the University of Tromsø.

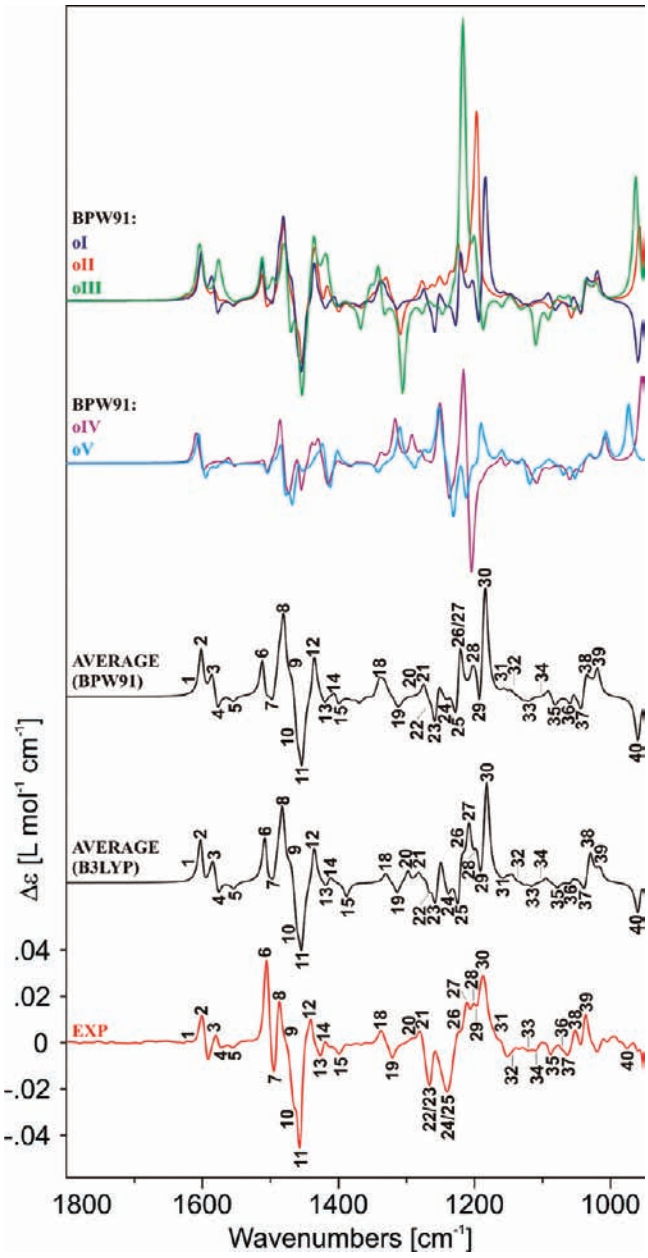

Figure 3. Experimental VCD spectrum of **ORTHO** together with calculated spectra at the BPW91/6-31G** and B3LYP/6-31G** levels, obtained as a population-weighted average of the spectra of five conformers. VCD spectra of the five conformers calculated by BPW91 are also presented.

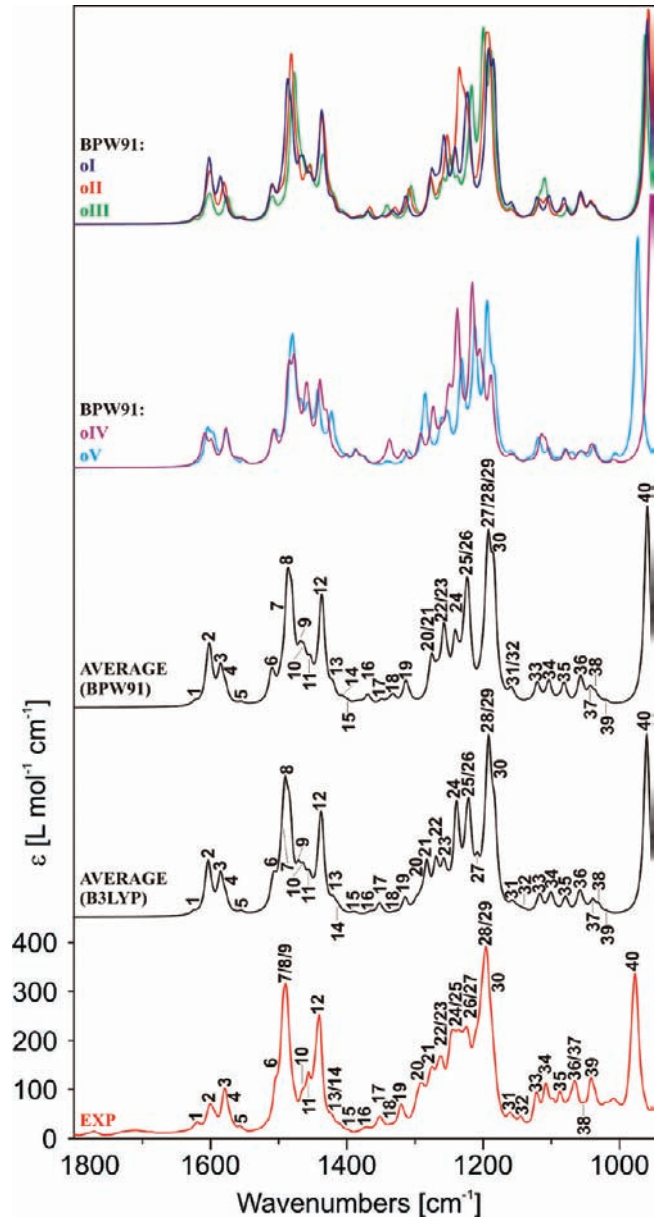

Figure 4. Experimental IR absorption spectrum of **ORTHO** together with calculated spectra at the BPW91/6-31G** and B3LYP/6-31G** level, obtained as a population-weighted average of the spectra of five conformers. VCD spectra of the conformers calculated by BPW91 are also presented.

Results

Conformational Analysis. Binaphthyl derivatives with phenyl groups substituted in the ortho position were assumed from the synthesis[15] to have (*R*)-configuration at the naphthyl−naphthyl stereogenic axis. Conformational analysis and subsequent DFT optimization at the B3LYP/6-31G** and BPW91/6-31-G** levels revealed five conformers (Figure 1), three of them (**oI**, **oII**, and **oIII**) possessing (*R*,*S*,*S*) configuration and two of them (**oIV** and **oV**) having (*R*,*R*,*S*) configuration of the naphthyl−naphthyl, naphthyl(1)−phenyl(1), and naphthyl(2)−phenyl(2) stereogenic axes, respectively. The calculated energetic barrier for the hindered rotation about the naphthyl−phenyl bond, changing the absolute configuration of this stereogenic axis, is less than 22 kcal mol^{-1}. Therefore, we consider geometries with (*R*,*S*,*S*) configuration (**oI**, **oII**, and **oIII**) and geometries with (*R*,*R*,*S*) configuration (**oIV** and **oV**) to be interconvertible conformers.[27] Calculations of the relative abundance of all conformers according to their ΔG values obtained by both DFT methods (Table 1) showed that only **oI** and **oII** are significantly populated at room temperature with relative populations of approximately 85% and 14%, respectively, while the relative abundance of **oIII** is less than 0.2% and the relative population of **oIV** and **oV** is close to zero ($\ll$0.1%). The dihedral angles between the naphthyl−naphthyl, naphthyl(1)−phenyl(1), and naphthyl(2)−phenyl(2) planes are summarized for all the B3LYP and BPW91 optimized structures in Table 2.

The conformational search of the binaphthyl derivative with phenyl groups substituted in the meta position was done assuming that an (*S*)-configuration of the naphthyl−naphthyl stereogenic axis is given from synthesis. The following DFT optimization at the B3LYP/6-31G** and BPW91/6-31-G** levels led to four conformers in the case of BPW91 (Figure 2), two of them possessing (*S*,*R*,*R*) configuration (**mI** and **mII**) and

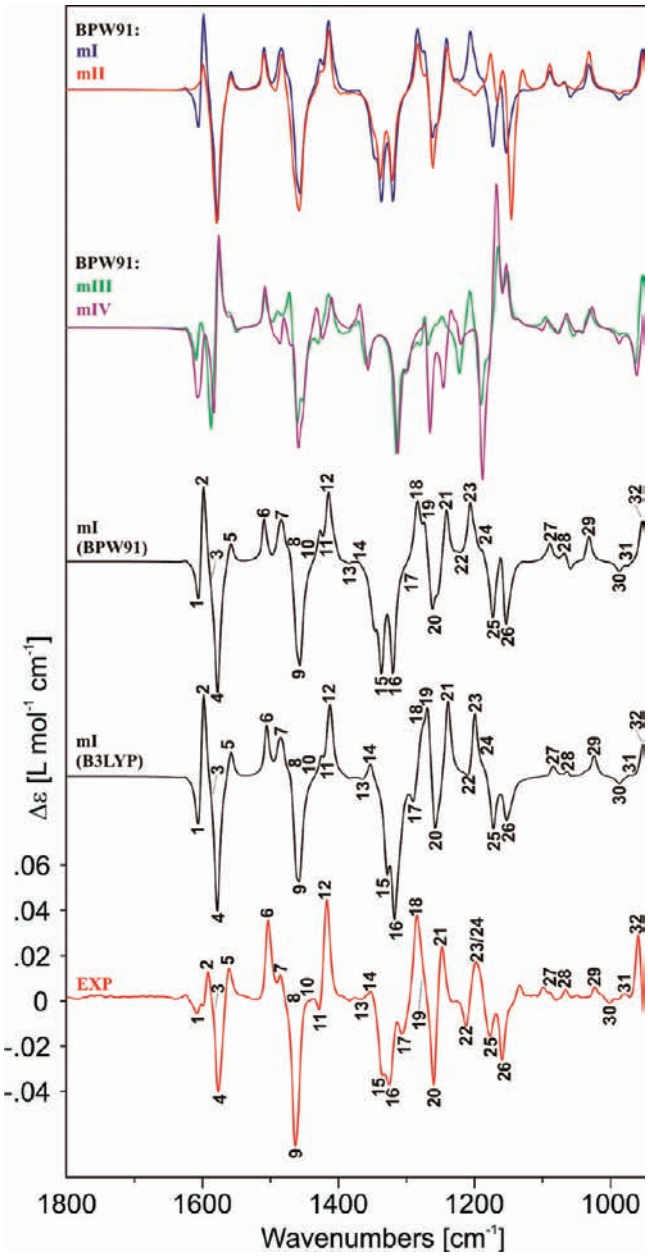

Figure 5. Experimental VCD spectrum of **META** together with calculated spectra of **mI** at the BPW91/6-31G** and B3LYP/6-31G** level. VCD spectra of the conformers calculated by BPW91 are also presented.

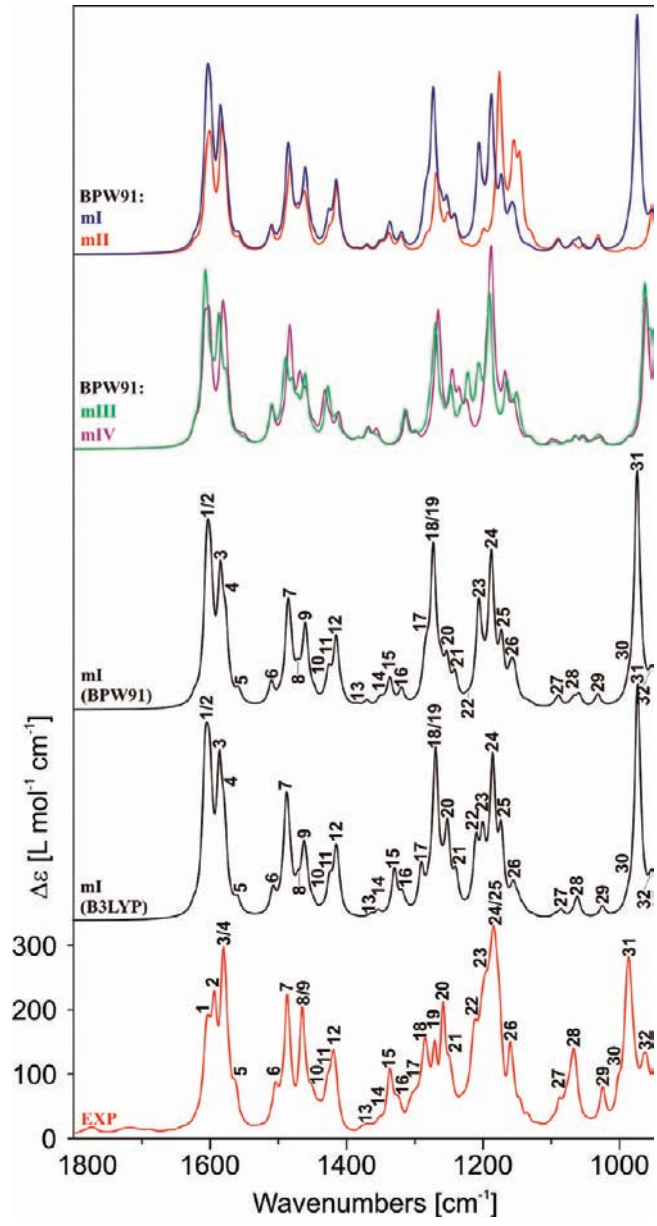

Figure 6. Experimental IR absorption spectrum of **META** together with calculated spectra of **mI** at the BPW91/6-31G** and B3LYP/6-31G** levels. VCD spectra of the conformers calculated by BPW91 are also presented.

two of them (*S*,*S*,*R*) configuration (**mIII** and **mIV**). As in the case of **ORTHO**, the energy needed to cross the energetic barrier to change the configuration at the naphthyl−phenyl stereogenic axis is less than 22 kcal mol^{-1} and therefore we can consider geometries with (*S*,*R*,*R*) configuration (**mI** and **mII**) and geometries with (*S*,*S*,*R*) configuration (**mIII** and **mIV**) to be interconvertible conformers. According to the calculated ΔG values of all conformers (Table 3), only **mI** is significantly populated at room temperature. The relative abundance of the other conformers is negligible ($\ll$0.1%). In the case of B3LYP, the geometry of **mIV** does not represent an energetic minimum and the optimization of this structure at the B3LYP/6-31G** level converges to a geometry identical with the **mI** conformation. Nonetheless, this fact does not affect the results because the BPW91/6-31G** geometry of **mIV** is energetically unfavorable and therefore not populated at room temperature. Dihedral angles of all conformers of **META** on the three stereogenic axes are summarized in Table 4.

VCD and IR Spectra. Figure 3 shows the experimental VCD spectrum of **ORTHO** together with the weight-averaged spectra of all conformers, calculated according to their relative abundance, by both BPW91 and B3LYP methods. To demonstrate the differences between the VCD spectra of the five conformers, spectra of **oI**−**oV** calculated by BPW91 are also displayed. It is evident from Figure 3 that the structures **oIV** and **oV**, which show negligible relative populations, possess VCD spectral patterns that do not agree with the experimental spectra. The same comparison for the IR absorption spectra is presented in Figure 4. Bands in the calculated and experimental spectra were identified and numbered. An excellent agreement with the experimental spectrum in terms of positions and relative intensities of all the identified bands can be observed for the computed spectra by using both hybrid B3LYP and nonhybrid BPW91 functionals.

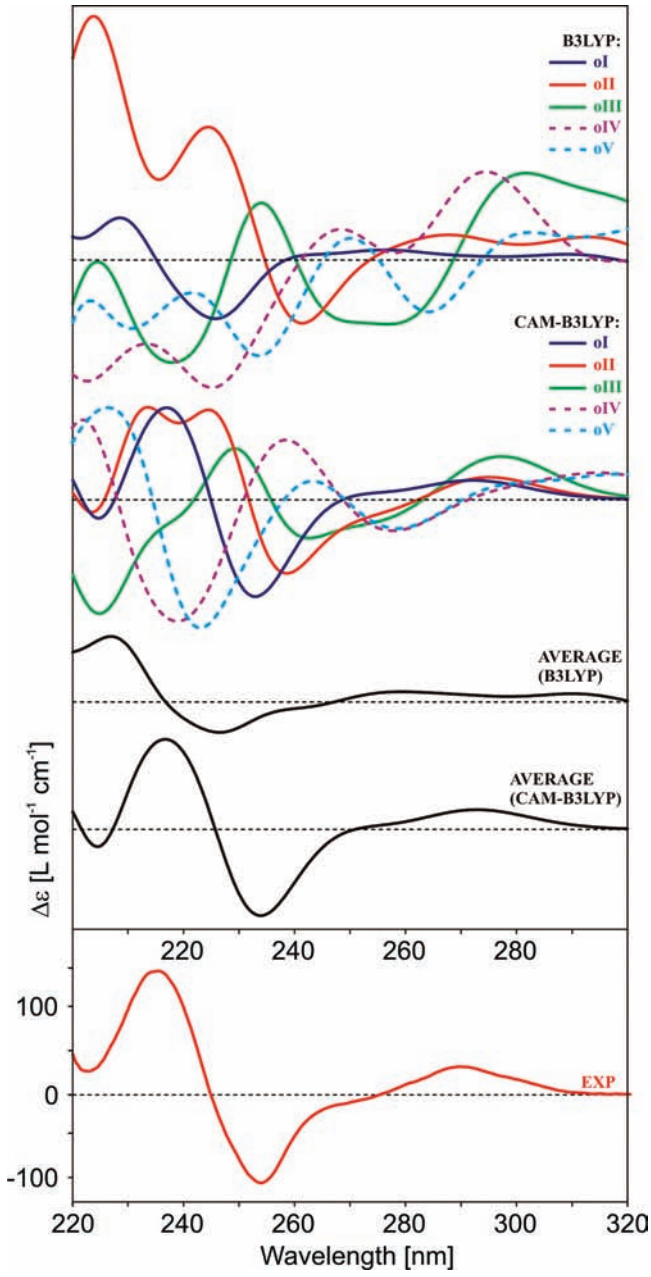

Figure 7. ECD spectra of the conformers of **ORTHO** calculated by using B3LYP and CAM-B3LYP functionals ((*R*,*S*,*S*), full lines; (*R*,*R*,*S*), broken lines). Comparison of population-weighted average of spectra of all the conformers with the experimental ECD spectrum.

A similar comparison of calculated and experimental VCD and IR absorption spectra of **META** is presented in Figure 5 and Figure 6, respectively. Despite the fact that **mI** is the only significantly populated conformer, spectra of **mII**, **mIII**, and **mIV** calculated by BPW91 are also shown to demonstrate their differences from **mI** and from the experimental spectrum. The experimental spectrum was compared with the calculated spectrum of **mI**, the only significantly populated conformer at room temperature, and then the identification and numbering of the bands in the calculated and experimental spectra was done. Again, an excellent agreement of theoretical and experimental spectra in terms of positions and relative intensities of all the identified bands can be seen for both DFT functionals. Generally, there is not a big difference in the quality of the calculated VCD spectra with use of either the B3LYP or the BPW91 functional, as both of them describe perfectly all identifiable vibrational transitions in the spectra.

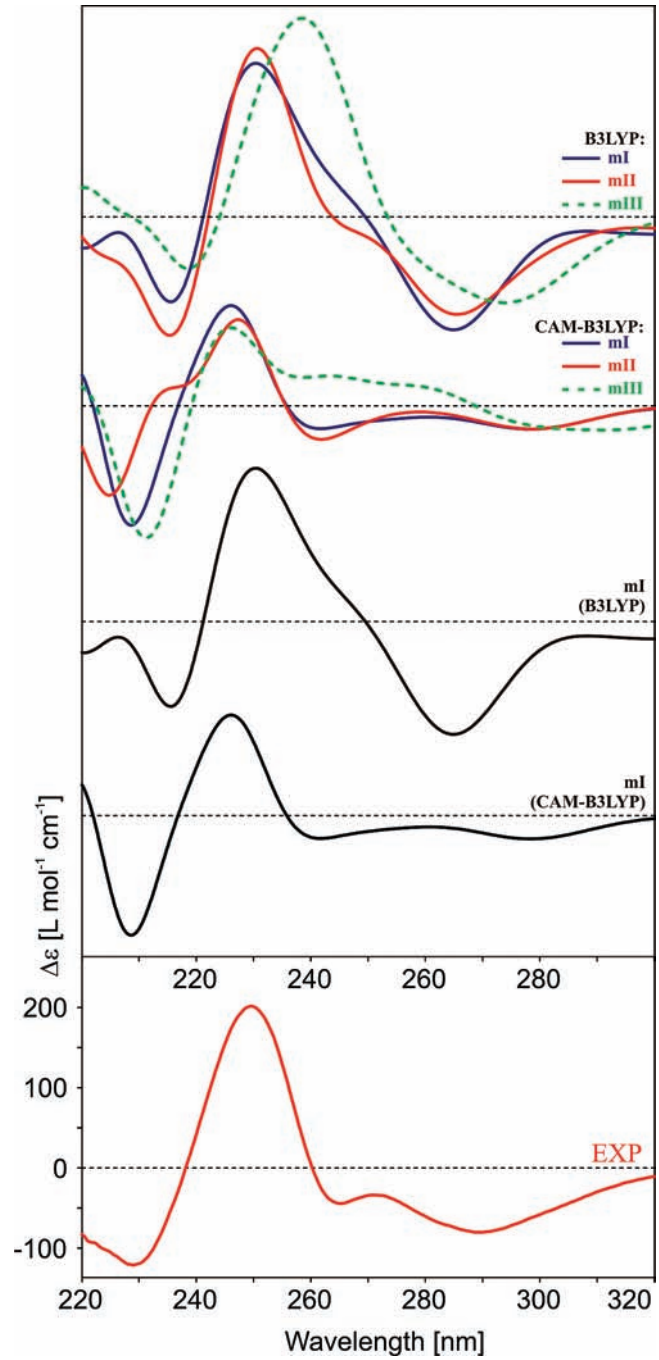

Figure 8. ECD spectra of the three stable conformers of **META** calculated by using B3LYP and CAM-B3LYP functionals ((*S*,*R*,*R*), full lines; (*S*,*S*,*R*), broken line). Comparison of calculated spectrum of the only populated **mI** with the experimental ECD spectrum.

ECD Spectra. Figure 7 shows the ECD spectra of all conformers of **ORTHO** together with their population-weighted average, calculated by B3LYP and CAM-B3LYP, and compared to the experimental ECD spectrum. An excellent agreement can be observed for the population-weighted averaged spectrum computed by using the CAM-B3LYP functional while the results of the B3LYP calculations are inferior but still in a good agreement. To describe the spectral pattern of the experimental ECD spectrum in the given spectral region, it was necessary to employ more electronic transitions when using the B3LYP compared to CAM-B3LYP functional (see Figure S1 in the Supporting Information).

The calculated ECD spectra of all conformers of **META** and the comparison of the experimental spectrum with the spectrum

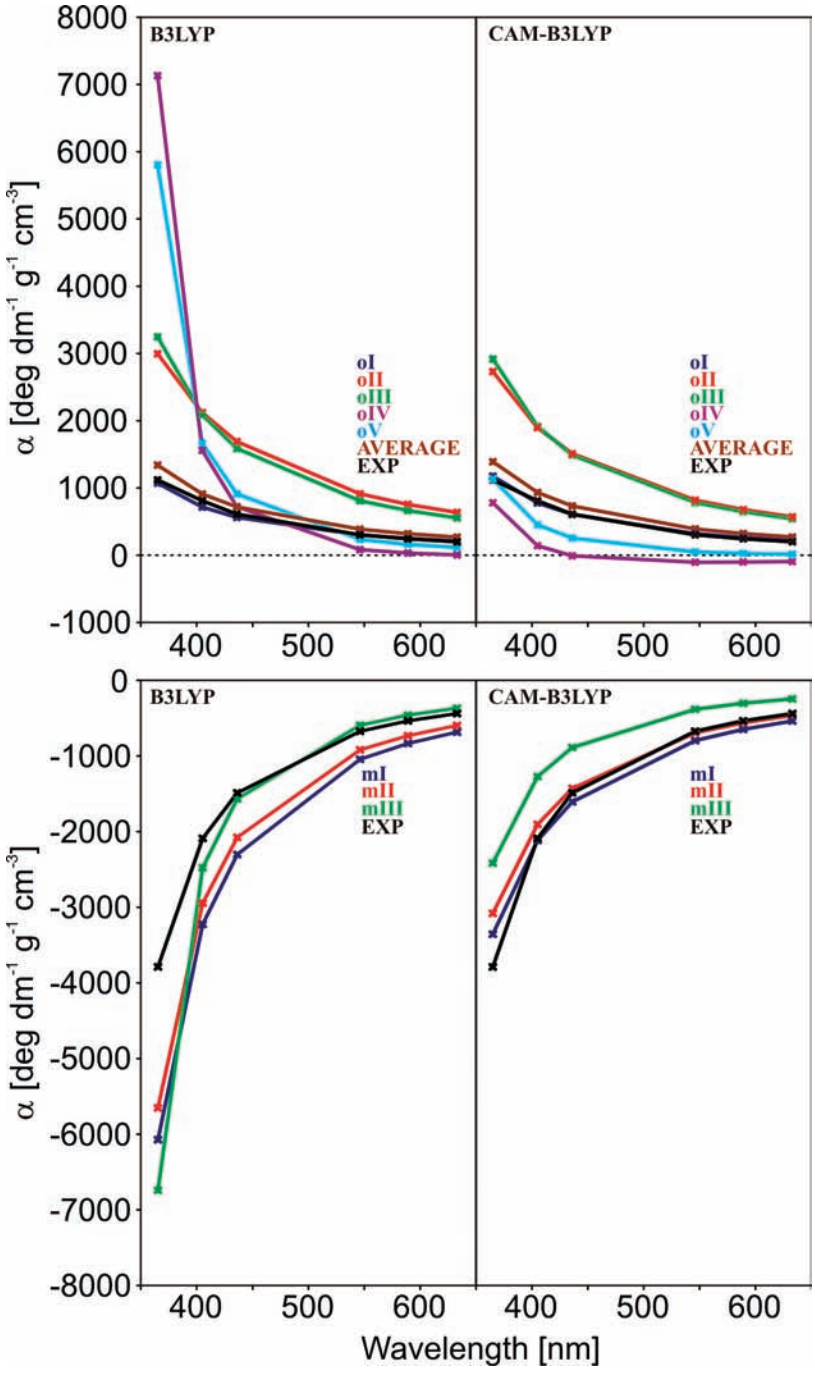

Figure 9. Experimental OR of **ORTHO** (top) and **META** (bottom) compared with calculated values for all conformers and their population-weighted average.

of **mI** being the exclusively abundant conformer is presented in Figure 8. Again, the agreement between experimental and calculated data is better for CAM-B3LYP and this DFT functional appears to more faithfully describe the lowest excited states of the molecule, as a much higher number of excited states need to be included in the B3LYP calculations (see Figure S2 in the Supporting Information).

Transparent Spectral Region Optical Rotation. Figure 9 shows the experimental optical rotations of **ORTHO** for six wavelenghts in transparent wavelength range together with the calculated values for all conformers and their population-weighted average. Both B3LYP and CAM-B3LYP functionals offer an excellent agreement with the experimental optical rotation values for all measured wavelengths. Exact values of all calculated and experimental optical rotations for both DFT functionals are summarized in Table 5.

Experimental optical rotations of **META** together with calculated rotations of all conformers are also shown in Figure 9. Experimental optical rotation values and calculated values of **mI** are in a good agreement for CAM-B3LYP while B3LYP slightly overestimates the experimental values. Table 6 shows the calculated optical rotations for both functionals together with experimental data.

Discussion

A perfect agreement between experimental and calculated OR, IR, VCD, and ECD for both **ORTHO** and **META** indicates

TABLE 5: Specific Optical Rotation of the Five Conformers of ORTHO and Their Population-Weighted Average Calculated at the B3LYP/6-311G and CAM-B3LYP/6-311G** Levels Together with Experimental Values**

	$[\alpha]_{365}$		$[\alpha]_{405}$		$[\alpha]_{436}$		$[\alpha]_{546}$		$[\alpha]_{589}$		$[\alpha]_{633}$	
conformer	B3LYP	CAMB3LYP	B3LYP	CAMB3LYP	B3LYP	CAMB3LYP	B3LYP	CAMB3LYP	B3LYP	CAMB3LYP	B3LYP	CAMB3LYP
oI	1073.0	1174.5	716.6	777.9	562.7	607.6	302.0	321.0	250.2	264.9	210.6	222.2
oII	2995.2	2730.4	2120.7	1896.4	1688.9	1509.6	912.5	819.0	755.2	678.7	634.5	570.9
oIII	3246.5	2917.2	2088.6	1914.2	1587.7	1490.0	809.4	783.8	664.9	646.6	556.1	542.2
oIV	5806.7	1132.2	1664.9	452.6	911.5	255.0	234.1	48.6	161.2	26.5	115.9	13.6
oV	7130.9	779.5	1559.6	141.3	720.3	−8.5	83.2	−104.2	32.2	−101.3	5.3	−94.5
av	1338.8	1389.6	910.5	932.4	718.1	732.2	386.1	389.7	319.8	322.0	269.0	270.3
exptl	1120.0		810.0		610.0		303.1		244.0		200.0	

TABLE 6: Specific Optical Rotation of the Four Conformers of META and Their Population-Weighted Average Calculated at the B3LYP/6-311G and CAM-B3LYP/6-311G** Levels Together with Experimental Values**

	$[\alpha]_{365}$		$[\alpha]_{405}$		$[\alpha]_{436}$		$[\alpha]_{546}$		$[\alpha]_{589}$		$[\alpha]_{633}$	
conformer	B3LYP	CAMB3LYP	B3LYP	CAMB3LYP	B3LYP	CAMB3LYP	B3LYP	CAMB3LYP	B3LYP	CAMB3LYP	B3LYP	CAMB3LYP
mI	−6072.9	−3356.1	−3225.8	−2116.5	−2302.0	−1606.4	−1043.9	−797.3	−835.6	−648.4	−684.7	−537.5
mII	−5652.7	−3081.0	−2944.9	−1904.9	−2077.5	−1430.5	−919.2	−694.5	−731.7	−562.0	−596.9	−464.1
mIII	−6741.8	−2416.1	−2475.9	−1271.4	−1565.3	−889.2	−593.5	−383.1	−460.1	−303.0	−368.1	−245.9
av	−6072.9	−3356.1	−3225.8	−2116.5	−2302.0	−1606.4	−1043.9	−797.3	−835.6	−648.4	−684.7	−537.5
exptl	−3789.0		−2089.0		−1488.0		−674.0		−536.0		−440.0	

that the studied binaphthyl system is well-described by DFT. Among the methods used in this work, VCD spectroscopy proved to be the most sensitive and unambiguous method for the determination of absolute configuration and the molecular geometry. A band-to-band assignment of experimental and calculated VCD spectra of **ORTHO** and **META** confirms the correct determination of the molecular geometry of both binaphthyl derivatives. However, slightly better results were achieved for **META**. This conclusion is not very surprising, as the final VCD spectrum of **META** is in fact a spectrum of the single conformer **mI**, while the final spectrum of **ORTHO** is a weighted average of two subspectra of the two significantly populated **oI** and **oII** conformers, for which there is an uncertainty arising from the calculations of their relative abundance, a calculation having larger uncertainties than the calculation of the VCD spectrum for a single conformation. In contrast, the energetic gap between the **mI** and **mII** conformers causes **mI** to be the only conformer significantly populated at room temperature with negligible abundance of other conformers that could affect the resulting spectrum. The extent of agreement between experimental and calculated VCD spectra is equal for both the nonhybrid BPW91 and hybrid B3LYP functionals. This statement is in disagreement with a previous study of binaphthyl systems where the results of BPW91 showed better agreement to experiment than the data obtained by using B3LYP and the MPW1PW91 functionals.[13]

The combination of experimental ECD with ab initio calculated spectra for determining the molecular geometry has usually been less convincing in comparison to VCD, as ECD can suffer from many problems such as a high density of electronic transitions preventing their resolution, the occurrence of transitions with non-Gaussian profiles, or the presence of bands with nonuniform width. However, the agreement of the experimental and calculated ECD spectra was surprisingly good, especially in the case of **ORTHO**. Comparing the B3LYP and CAM-B3LYP results, the long-range corrected hybrid functional CAM-B3LYP offers far superior results.

The results of the calculation of the optical rotation in the transparent spectral region revealed that this method is not able to distinguish between the individual conformers but can be successfully used to prove the absolute configuration of the molecule. The comparison of calculated and experimental optical rotations confirmed that the configuration of the naphthyl−naphthyl stereogenic axis is (*R*) in the case of **ORTHO** and (*S*) in the case of **META**.

Conclusions

Absolute configuration at the stereogenic axes of the two BINOL bis-phenylene phosphoramidites and prevailing solution conformations were studied by OR, IR, ECD, and VCD methods combined with ab initio calculations. It was unambiguously determined that **ORTHO** occurs in three conformations **oI**, **oII**, and **oIII**, with relative populations of 85%, 15%, and <1% (according to B3LYP) or 86%, 14%, and <1% (according to BPW91), respectively, at room temperature. The absolute configuration at the naphthyl−naphthyl, naphthyl(1)−phenyl(1), and naphthyl(2)−phenyl(2) stereogenic axes was determined as (*R*,*S*,*S*) for all three conformers **oI**, **oII**, and **oIII**. The dihedral angle of the naphthyl−naphthyl axis of the dominant **oI** and **oII** conformers with their overall abundance >99% is very similar, −96° and −99° for **oI** and **oII**, respectively. For the **META** derivative, only one conformer **mI** populated at room temperature was found, with absolute configuration of the forementioned stereogenic axis determined as (*S*,*R*,*R*). The dihedral angle of the naphthyl−naphthyl axis of **mI** was determined as ∼77°. An excellent agreement between experimental and calculated OR, IR, ECD, and VCD data for both **ORTHO** and **META** fully supports this conclusion. Concerning the DFT functionals used in this study, both hybrid B3LYP and nonhybrid BPW91 showed excellent results for the calculation of the VCD spectra. Long-range CAM-B3LYP apparently performed better than the common B3LYP functional in the calculation of ECD, while the results for both functionals in the calculation of OR were comparable.

Acknowledgment. We thank Dr. Maxime Guillaume (University of Tromsø, Norway) for helping with the project and for valuable discussions. We are grateful to Lucie Holasová, MSc and Štefan Štanga, MSc (Analytical laboratory, Institute of Organic Chemistry and Biochemistry, Prague, Czech Republic) for transparent spectral region optical rotation measurements. We also acknowledge the CTCC (University of Tromsø, Norway) and Computer Center (ICT Prague, Czech Republic)

for providing the access to computational resources. The work was supported by research grant MSM6046137307 from the Ministry of Education, Youth, and Sports of the Czech Republic and the Slovak Grant Agency for Science (grant No. 1/0265/09). K.R. has received support from the Research Council of Norway through CoE (Grant No 179568/V30) and YFF (Grant No 162746/V00) grants, as well as a grant of computer time from the supercomputing program.

Supporting Information Available: Electronic transitions and ECD spectra of the conformers of **ORTHO** and **META** calculated by B3LYP and CAM-B3LYP functionals. This material is available free of charge via the Internet at http://pubs.acs.org.

References and Notes

(1) Brunel, J. M. *Chem. Rev.* **2008**, *108*, 1170.
(2) Yamada, K.; Tomioka, K. *Chem. Rev.* **2008**, *108*, 2874.
(3) Alexakis, A.; Backvall, J. E.; Krause, N.; Pamies, O.; Dieguez, M. *Chem. Rev.* **2008**, *108*, 2796.
(4) Jerphagnon, T.; Pizzuti, M. G.; Minaard, A. J.; Feringa, B. L. *Chem. Soc. Rev.* **2009**, 1039.
(5) RajanBabu, T. V. *Chem. Rev.* **2003**, *103*, 2845.
(6) Najera, C.; Sansano, J. M. *Chem. Rev.* **2007**, *107*, 4584.
(7) Polavarapu, P. L.; Jeirath, N.; Walia, S. *J. Phys. Chem. A* **2009**, *113*, 5423.
(8) Di Bari, L.; Pescitelli, G.; Salvadori, P. *J. Am. Chem. Soc.* **1999**, *121*, 7998.
(9) Mason, S. F.; Seal, R. H.; Roberts, D. R. *Tetrahedron* **1974**, *30*, 1671.
(10) Stephens, P. J.; Pan, J. J.; Devlin, F. J.; Urbanova, M.; Julinek, O.; Hajicek, J. *Chirality* **2008**, *20*, 454.
(11) Stephens, P. J.; Devlin, F. J.; Pan, J. J. *Chirality* **2008**, *20*, 643.
(12) Devlin, F. J.; Stephens, P. J.; Cheeseman, J. R.; Frisch, M. J. *J. Phys. Chem. A* **1997**, *101*, 6322.
(13) Setnicka, V.; Urbanova, M.; Bour, P.; Kral, V.; Volka, K. *J. Phys. Chem. A* **2001**, *105*, 8931.
(14) Polavarapu, P. L. *Chirality* **2008**, *20*, 664.
(15) Miklášová, N.; Julínek, O.; Mešková, M.; Setnička, V.; Urbanová, M.; Putala, M. *Eur. J. Org. Chem.* In preparation.
(16) Urbanová, M.; Setnička, V.; Volka, K. *Chirality* **2000**, *12*, 199.
(17) HyperChem 8, www.hyper.com.
(18) Gaussian 03, www.gaussian.com.
(19) Dalton 2.0, www.kjemi.uio.no/software/dalton.
(20) Yanai, T.; Tew, D. P.; Handy, N. C. *Chem. Phys. Lett.* **2004**, *393*, 51.
(21) Cai, Z. L.; Crossley, M. J.; Reimers, J. R.; Kobayashi, R.; Amos, R. D. *J. Phys. Chem. B* **2006**, *110*, 15624.
(22) Jacquemin, D.; Perpete, E. A.; Adamo, C. *THEOCHEM* **2008**, *863*, 123.
(23) Jacquemin, D.; Perpete, E. A.; Scuseria, G. E.; Ciofini, I.; Adamo, C. *J. Chem. Theory Comput.* **2008**, *4*, 123.
(24) Peach, M. J. G.; Benfield, P.; Helgaker, T.; Tozer, D. J. *J. Chem. Phys.* **2008**, 128.
(25) Peach, M. J. G.; Le Sueur, C. R.; Ruud, K.; Guillaume, M.; Tozer, D. J. *Phys. Chem. Chem. Phys.* **2009**, *11*, 4465.
(26) Shcherbin, D.; Ruud, K. *Chem. Phys.* **2008**, *349*, 234.
(27) Leroux, F. *ChemBioChem* **2004**, *5*, 644.

JP906724F